Excited-State Kinetics of the Carotenoid S_1 State in LHC II and Two-Photon Excitation Spectra of Lutein and β-Carotene in Solution: Efficient Car $S_1 \rightarrow$Chl Electronic Energy Transfer via Hot S_1 States?†

Peter J. Walla, Patricia A. Linden, Kaoru Ohta, and Graham R. Fleming*

Department of Chemistry, University of California at Berkeley, and Physical Biosciences Division, Lawrence Berkeley National Laboratory, Berkeley, California 94720

Received: April 19, 2001; In Final Form: June 26, 2001

The excited-state dynamics of the carotenoids (Car) in light-harvesting complex II (LHC II) of *Chlamydomonas reinhardtii* were studied by transient absorption measurements. The decay of the Car S_1 population ranges from ~200 fs to over 7 ps, depending on the excitation and detection wavelengths. In contrast, a 200 fs Car $S_1 \rightarrow$Chlorophyll (Chl) energy transfer component was the dominant time constant for our earlier two-photon fluorescence up-conversion measurements (Walla, P. J.; et al. *J. Phys. Chem. B* **2000**, *104*, 4799−4806). We also present the two-photon excitation (TPE) spectra of lutein and β-carotene in solution and compare them with the TPE spectrum of LHC II. The TPE-spectrum of LHC II has an onset much further to the blue and a width that is narrower than expected from comparison to the S_1 fluorescence of lutein and β-carotene in solution. Different environments may affect the shape of the S_1 spectrum significantly. To explain the blue shift of the TPE spectrum and the difference in the time constants obtained from two-photon vs one-photon methods, we suggest that a major part of the Car $S_1 \rightarrow$Chl electronic energy transfer (EET) is due to efficient EET from hot vibronic states of the Cars. We also suggest that the subpicosecond kinetics has a very broad distribution of EET time scales due to EET from hot states.

1. Introduction

The most abundant light-harvesting protein of green algae and higher plants is the light-harvesting complex II (LHC II).[21,22,43] Over half the light used for photosynthesis is collected by the chromophores in this protein. In the thylakoid membranes of chloroplasts, LHC II serves as the primary donor of electronic excitation energy, which is funneled to the reaction centers and finally converted into chemically storable energy.

Each LHC II monomer contains 7 or 8 chlorophyll *a* (Chl *a*), 5 or 6 chlorophyll *b* (Chl *b*), and roughly 3 or 4 carotenoid (Car) molecules. The Cars present in an LHC II monomer are roughly 2 luteins, 1 neoxanthin, and varying substoichiometric amounts of violaxanthin (Figure 1).[22,32,41] In the 3.4 Å crystal structure of the LHC II from Kühlbrandt and co-workers, only 2 Cars are resolved.[24] They are surrounded by at least 7 Chl in van der Waals contact and 5 Chl in close proximity. Recent work of Bassi and co-workers and Hobe et al. showed that these two Car's sites have the highest affinity to lutein.[6,7,18] One of the central Car sites can also be occupied by a violaxanthin. The other resolved site shows affinity only to lutein whereas an unresolved third site has affinity to neoxanthin.[7,35] A fourth site is probably exclusively occupied by violaxanthin. It was recently shown by Ruban et al. that approximately one violaxanthin is bound per monomeric subunit of LHC II.[36]

The main function of the Chls is light-harvesting in the blue (Soret-transitions) and the red (Q_y and Q_x transitions) regions of visible light (Figure 2). In contrast, the function of the carotenoids is at least 3-fold: they serve as light-harvesting molecules in the blue-green region, they quench Chl triplet states to prevent the creation of dangerous singlet oxygen, and they play an important structural role. It has also been proposed that they serve an important function by regulating the flow of excessive excitation energy from the antenna to the photosystem II (PSII) reaction center.[12,19,37] The aim of the present work is

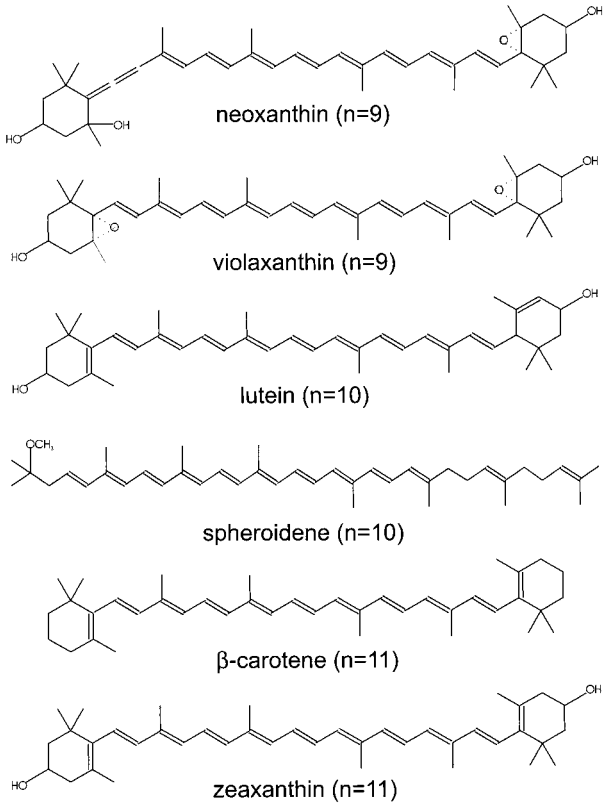

Figure 1. Molecular structures of the carotenoids mentioned in this work, where n = the number of conjugated double bonds in each.

† Part of the special issue "Noboru Mataga Festschrift".

10.1021/jp011495x CCC: $22.00
Published on Web 08/01/2001

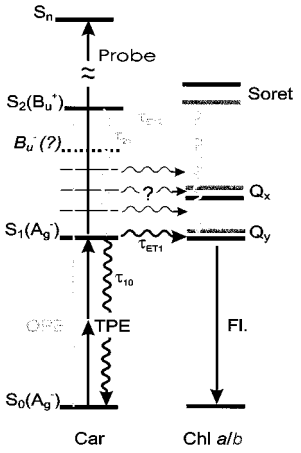

Figure 2. Energy level diagram for carotenoids and chlorophylls in LHC II. Black arrows: energy pathways occurring in the TPE pump−probe experiment. Gray arrows: Additional energy pathways in conventional one-photon experiments. OPE: one-photon excitation. TPE: two-photon excitation. Fl: Fluorescence. τ_{ET2}: time constant for Car $S_2 \rightarrow$Chl EET ($\sim$100 fs).[5,17,46] τ_{21}: time constant for Car $S_2 \rightarrow S_1$ IC ($\sim$ 200 fs).[16] τ_{ET1}: time constant for Car $S_1 \rightarrow$Chl EET. τ_{10}: time constant for Car $S_1 \rightarrow S_0$ IC. $\tau_{S1} = (\tau_{ET1} - 1 + \tau_{10}^{-1})^{-1}$ lifetime of the Car S_1 state measured in this work.

to investigate the first mentioned function, the mechanism of light-harvesting by carotenoids in LHC II.

It is known that the electronic energy transfer (EET) of singlet excitation from Cars to Chls is very efficient ($\sim$80%).[5,41] The Cars possess at least two states corresponding to transitions in the visible region: S_2, which is located just below the Chl *b* Soret-transition at $\sim$20000 cm^{-1} and S_1, which has an energy similar to the Chl Q_y-transitions ($\sim$15000 cm^{-1}) (Figure 2). Recently, the presence of another singlet state, located between what have traditionally been called the S_1 and S_2 states, has been suggested by Sashima et al.[39] However, from the ground state only the transition to S_2 has a significant transition dipole moment; therefore, only S_2 can contribute to the primary light-harvesting of Cars. To explain this, the electronic states of carotenoids are often described by analogy to polyenes. Their ground state (S_0) and first excited state (S_1) both possess A_g^- symmetry, their newly identified excited state has been assigned a B_u^- symmetry,[39] and their second excited state (S_2) possesses B_u^+ symmetry in the idealized C_{2h} point group. Carotenoids do not adhere strictly to C_{2h} symmetry but still possess many of the spectral characteristics of the parent polyenes from which they were derived. Therefore, according to the selection rules for optical transitions, only the $S_0 \leftrightarrow S_2$ transition is optically dipole-allowed and contributes significantly to the absorption spectrum of Cars. However, it is known from studies of Cars in solution that after excitation into the S_2 state, they undergo rapid internal conversion (IC) in $\sim$200 fs to the S_1 state. The newly identified B_u^- state may facilitate this fast IC.[27] In the light-harvesting complex, starting at the Car S_2 state, the energy can generally flow via two pathways (Figure 2): One pathway, is a fast EET directly from the Car S_2 to Chl *a* and *b* states, with time constant τ_{ET2}, with subsequent relaxation to the Chl *a* Q_y state (Car $S_2 \rightarrow$Chl Q_x,Q_y). The other pathway is first IC from S_2 in about 200 fs (τ_{21}) to S_1 and then EET from S_1 to Chl Q_y with time constant τ_{ET1} (Car $S_2 \rightarrow$Car $S_1 \rightarrow$Chl Q_y). Recently, we determined the branching between these two energy transfer pathways by measuring the lifetime of the Car S_2 state ($\tau_{S2} \sim 120 \pm 50$ fs) to be $\sim 50 \pm 10\%$ via S_2 and $\sim 30 \pm 10\%$ via S_1.[46] Twenty percent of the excitation energy is lost via Car $S_1 \rightarrow$Car S_0 internal conversion.[5,41]

In the same study, we determined the onset of the S_1 states of the Cars which are able to transfer their excitation energy to the Chls ($\sim$15100 $\pm$ 300 cm^{-1}) and a dominant EET time constant starting from the Car S_1 state ($\sim 250 \pm 50$ fs) by time-resolved and steady-state fluorescence measurements of the Chls after two-photon excitation of the Car S_1 states.[46] Of course, these measurements give information exclusively about the Cars that are able to transfer their S_1 excitation energy to the Chls.

To explore the Cars which do not transfer their energy to the Chls, we measured Car S_1 kinetics by detecting the strong S_1-S_n transition. Cars have very strong S_1 excited state absorption (ESA) usually in the region around 540 nm where very little ground-state absorption is found in LHC II. In addition to the 250 ± 50 fs Car $S_1 \rightarrow$ Chl EET component, we found several slower Car S_1 lifetimes. To elucidate which of the carotenoids in LHC II are participating in the EET from the Car S_1 state, we measured the two-photon excitation (TPE)-spectra of lutein and β-carotene in solution via the strong Car $S_1 \rightarrow S_n$ ESA. Comparison of these spectra with the TPE-spectrum of LHC II obtained by fluorescence detection suggests that a significant portion of the Car $S_1 \rightarrow$Chl EET could be due to efficient EET from higher vibronic states of the Cars.

2. Materials and Methods

LHC II was prepared from the PSI−PSII double-deficiency strain C2 of *Chlamydomonas reinhardtii* and purified using the methods described earlier.[1] Peripheral complexes such as CP24, CP26, and CP29 are not present, leaving only the major component of LHC II, often called LHC IIb, in the sample. HPLC calibration curves were created from known standards of lutein, neoxanthin, and violaxanthin. The Car composition measured was $\sim$2.0:0.9 lutein and loroxanthin:neoxanthin with substoichiometric amounts of violaxanthin ($\sim$0.5).[4] Lutein was dissolved in octanol by sonicating for $\sim$10 s and centrifuging for 4 min at $\sim$8000 *g*. β-Carotene (Acros) was dissolved in octane by sonicating and centrifuging in the same way. The samples were flowed through a 1 mm path-length quartz cell and maintained at 4−6 °C under a nitrogen atmosphere. To reduce scattering in the two-photon pump−probe experiments, a 0.45 μm filter was added to the flow cycle.

The pump−probe experiments were carried out as described previously.[45] Briefly, the pump pulses ($\sim$10 nJ, 85 fs fwhm, 250 kHz) and white-light probe pulses were both provided by a Coherent 9450 optical parametric amplifier. Excitation light intensity fluctuations were monitored with a power meter connected to a personal computer. In the one-photon pump−probe experiments, the pump pulses were compressed with a prism pair. The pump beam was focused with a $f = 10$ cm achromatic lens and the probe beam with a $f = 10$ cm lens. The probe wavelength was selected using a monochromator after the sample cell. Our instrument response function had a fwhm of <90 fs. For the two-photon experiments, we tried to minimize population created by the probe-white light by blocking the dominant 800 nm component with a highly reflective laser mirror and filtering the probe wavelength with a 550 nm interference filter prior to the sample cell. The pump beam was focused with an $f = 5$ cm achromatic lens and the probe beam with a $f = 10$ cm. Only about <25% of the intensity of both beams was blocked by a 50 μm pinhole. To suppress white-light fluctuations with a frequency similar to the pump-chopper frequency, a portion of the white light was measured with a separate photodiode and lock-in amplifier also triggered by the chopper. Subtracting this trace resulted in an improvement of the signal-to-noise ratio of more than a factor of 5. Previous

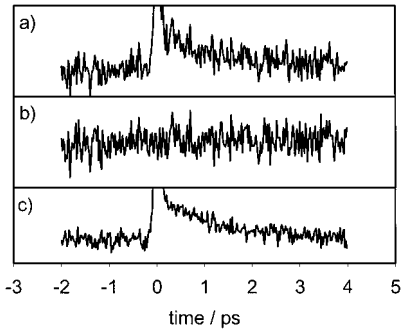

Figure 3. Two-photon pump−probe signal (λ_{exc} = 1350 nm, λ_{det} = 550 nm) for the carotenoid spheroidene in LH2 from *Rb. sphaeroides*.[45] (a) Without correction for white light fluctuations with a frequency similar to the chopper frequency. (b) Measured white light fluctuations. (c) Corrected trace.

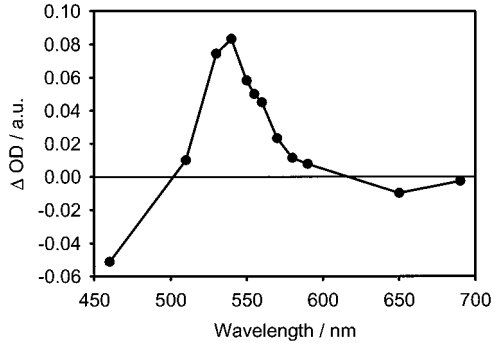

Figure 4. Transient absorption spectrum of LHC II at about 200 fs after excitation at 500 nm.

pump−probe data on the carotenoid spheroidene[45] is used to demonstrate this noise correction technique in Figure 3. In the two-photon pump−probe experiments, we always observed a very strong "coherent artifact". As an example of this effect, spheroidene shows an off-scale "coherent artifact" in Figure 3. The intensity of this artifact was proportional to the sample concentration and significantly stronger than in one-photon experiments using the same setup. The artifact had a quadratic dependence on the pump beam and was smaller for samples with a smaller two-photon cross-section (e.g., Chl *a* in solution). The origin of this artifact in two-photon pump probe experiments will be subject of future studies.

3. Results

3.1. Transient Absorption Kinetics after One-Photon Excitation of the Car S_2 State. In Figure 4 the ESA of LHC II in the Car $S_1 \rightarrow$ Car S_n region is shown at about 200 fs after excitation of the Car S_2/Chl *b* Soret region (λ_{Exc} = 500 nm). The ESA peaks at ~540 nm, which corresponds well with the findings of Frank et al. and other authors for isolated Cars in solution.[10,27,47] The ESA of the Car dominates over ground-state bleaching and ESA of the Chl resulting from direct excitation or EET from the Cars.

Transient absorption signals were measured at several probe wavelengths for both β-carotene in octane solution and LHC II. We fitted a function with four exponential components to most traces:

$$\Delta OD(t) = A_1 e^{-t/\tau_1} + A_2 e^{-t/\tau_2} + A_3 e^{-t/\tau_3} + A_4 e^{-t/\tau_4} \quad (1)$$

The fitting results are summarized in Table 1. A comparison of the kinetic traces for β-carotene and LHC II, both probed at 550 nm, is shown in Figure 5. Even though there is no

TABLE 1: Fitting Parameters for LHC II ESA

λ_{Exc}/nm	λ_{Det}/nm	τ_1/fs (A_1/%)	τ_2/fs (A_2/%)	τ_3/ps (A_3/%)	τ_4/ps (A_4/%)
500	530	52 (−100)[a]	*b*	3.9 (47)	33 (53)
500	540	7.7[c] (−67)[a]	105 (−33)[a]	3.2 (48)	28 (52)
490	550	130 (−100)	190 (62)	*d*	17 (38)
500	550	150 (−100)	220 (51)	4.0 (21)	24 (28)
510	550	83 (−100)	760 (1.5)	8.7 (63)	74 (25)
500	560	115 (−100)	170 (51)	3.3 (22)	25 (27)
500	570	42 (−100)	640 (15)	2.4 (34)	25 (51)
500	580	71 (−100)	631 (46)	*d*	16 (54)
500	590	90 (−100)	230 (61)	*d*	25 (39)

[a] These time constants are affected by a coherent artifact due to the similar excitation and detection wavelengths [b] For these traces the fitting algorithm was unable to separate τ_2 and τ_3. [c] This value was deconvoluted from a <90 fs instrument response function and has associated uncertainty. [d] For these traces the fitting algorithm was unable to separate τ_3 and τ_4.

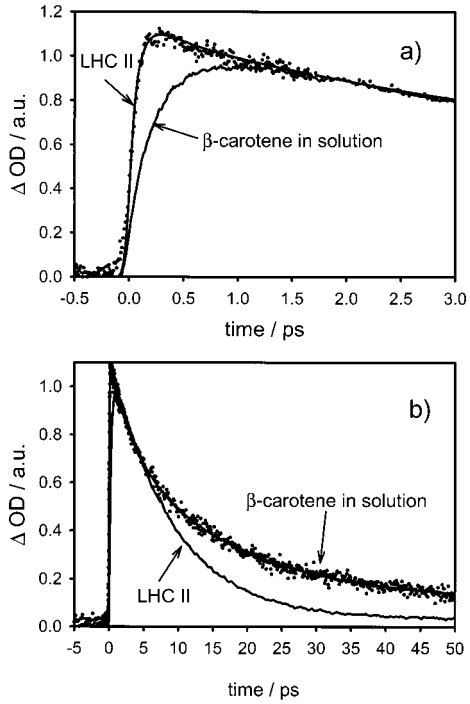

Figure 5. Transient absorption trace for β-carotene in octane solution (thin lines) and for LHC II (circles) along with exponential fits (thick lines, see Table 1 for parameters) (a) on a short time scale and (b) on a long time scale. λ_{Exc} = 500 nm; λ_{Det} = 550 nm.

β-carotene or other carotenoids electronically isomorphous to β-carotene in LHC II, β-carotene is used for comparison since there is extensive one-photon literature on this molecule and its characteristics are typical of carotenoids in solution. For β-carotene in octane, the transient absorption signal at 550 nm rises with a time constant of about 350 fs and decays on 9.0 ps time scale. The rise of the transient absorption signal results from S_2 to S_1 internal conversion, and the decay results from internal conversion from the S_1 to S_0 state. The results are consistent with previous measurements on β-carotene in solution.[27,47] However, the rise of the transient absorption for LHC II is significantly faster than for β-carotene. The signal decays with multiple time constants as shown in Table 1. Furthermore, the traces for LHC II differ strongly for different excitation and detection wavelengths. Because of the multiple electronic states involved, Table 1 should be predominantly regarded as a description of the transient absorption kinetics, which can be used for future analysis, e.g., when a more detailed crystal structure becomes available. Too much significance should not

be attached to the individual fitting parameters. We also believe that a global analysis fitting procedure is not appropriate to describe the population kinetics. Even with as many as four lifetimes, a global analysis procedure still yielded decay-associated spectra, which are a convolution of Car and Chl contributions (e.g. the sub-picosecond Chl→Chl EET components where convoluted with sub-picosecond Car→Chl EET components). However, the following general statements about the Car S_1 population still can be extracted from the data. (i) Depending on excitation and detection wavelengths, there is a significantly shorter rise time ($\tau_1 \sim 70-150$ fs) in the Car $S_1 \rightarrow$ Car S_n ESA compared to the IC time scale of lutein or other Cars in solution ($\sim$200 fs).[5] This rise is the mean lifetime, τ_{S2}, of different Car S_2-states and is shortened by the Car $S_2 \rightarrow$ Chl EET, τ_{ET2}. The observed rise time is in good agreement with our previous upconversion experiments ($\tau_{S2} \sim 120 \pm 50$ fs) indicating efficient Car $S_2 \rightarrow$ Chl EET.[46] The median of the observed τ_{S2} constants is at 90 fs, which yields an estimate for the Car $S_2 \rightarrow$ Chl EET efficiency of $\Phi_{ET1} = (\tau_{S2} - 1 - \tau_{21} - 1)\tau_{S2} \approx 60\%$ by assuming $\tau_{21} \approx 215$ fs.[16] The Car $S_1 \rightarrow$ Chl EET efficiency is then estimated to be $\Phi_{ET1} = \Phi_{OA} - \Phi_{ET2} \approx 20\%$ by assuming that the overall Car $\rightarrow$ Chl EET efficiency is $\Phi_{OA} \approx 80\%$.[5,14,41] (ii) In general, the decay components can be divided into components with significantly shorter lifetimes ($<5-10$ ps) than those observed for carotenoids in solution and longer components (≥ 10 ps) with lifetimes similar to the S_1 lifetimes of isolated Cars (such as 14.6 ps for lutein, 35 ps for neoxanthin, and 23−25 ps for violaxanthin).[10,33,34] The most straightforward explanation is that the shorter lifetimes result from a subpopulation of the Car states that transfer energy to the Chl via Car S_1, and that the longer lifetimes correspond to Car that do not participate in EET. (iii) A sub-picosecond decay (105 fs-760 fs), whose time constant depends on the pump and probe wavelengths, is seen at all detection wavelengths. In global analysis procedures, this component is usually convoluted with other sub-picosecond processes such as Chl→ Chl EET. This fast decay does not appear in the corresponding traces of the Cars in solution (see Figure 5); therefore, we do not attribute it to spectral evolution of the Car itself. However, the exact amplitude of this component is difficult to determine because the decay time scale is on the same order of magnitude as the rise component. The rise and decay components effectively overlap at short times, partially canceling each other's amplitude. So, any number of rise and decay amplitudes can be used to attain the same final fitting results. Therefore, no rise amplitude can reliably be assigned. However, the data cannot be fitted without a fast decay component. The time constants depend strongly on the excitation and probe wavelengths. With excitation at $\sim$500 nm, we observe a $\sim$200 fs component at 550, 560, and 590 nm, and a $\sim$630−640 fs component at 570 and 580 nm. A predominant 200 fs component can be seen for 490 nm excitation, and only a very small 700 fs component is present for 510 nm excitation.

For our previous two-photon excitation upconversion work,[46] the arrival of the excitation energy due to transfer from the directly populated Car S_1 state was measured by the rise of the Chl-fluorescence. The Chl-kinetics in this type of experiment were, of course, not dominated by the Car S_1 states with longer (>5 ps) lifetimes, because in those experiments, Chl is only populated from Car S_1 states which have efficient EET. The two-photon upconversion experiment is thus complementary to the regular one-photon pump−probe experiment of this work. The former is only sensitive to those Car S_1 states which show very efficient Car $S_1 \rightarrow$ Chl EET ($\tau_{ET1} < 1$ ps), and the latter is mostly sensitive to those Car S_1 states which do not show efficient Car $S_1 \rightarrow$ Chl EET ($\tau_{ET1} > 5$ ps).

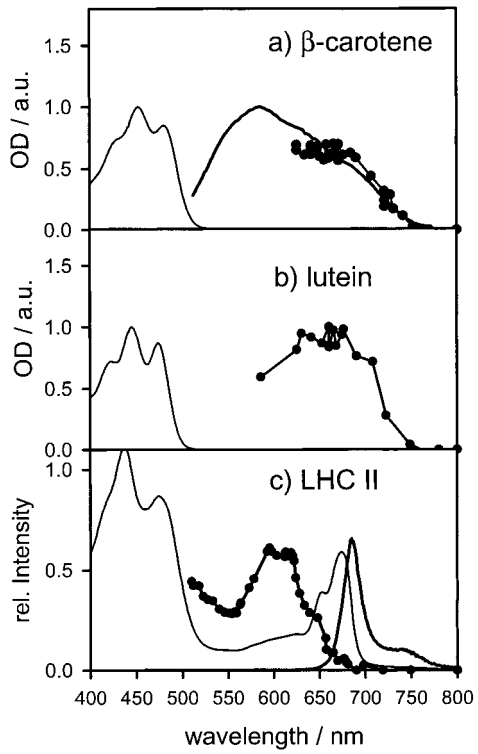

Figure 6. Two-photon excitation spectra (dots with solid lines) and absorption spectra (thin solid lines) of (a) β-Carotene in octane and (b) lutein in octanol monitored by Car $S_1 \rightarrow$ Car S_n ESA ($\lambda_{ESA} = 550$ nm) and (c) LHC II of *Chlamydomonas reinhardtii* monitored by the Chl fluorescence ($\lambda_{Fl} = 690$ nm) due to Car $S_1 \rightarrow$ Chl EET (thick solid line = fluorescence from Chl *a*).[44] For β-carotene, the mirror image of the S_1 fluorescence spectrum (thick solid line) is plotted in (a).[29]

3.2. Two-Photon Pump−Probe Experiments. In Figure 6a,b, the TPE pump−probe signals of β-carotene in octane and lutein (the most abundant Car in LHC II) in octanol are shown as a function of the TPE wavelength. The TPE spectra were constructed by taking the whole area under the kinetic curves for different excitation wavelengths. To avoid contributions from coherent artifacts, we used the temporal profiles of the pump−probe signals at times longer than 500 fs. The result of this measurement is a direct TPE spectrum of the Car S_1 state. Since the TPE spectra are featureless, we have not attempted to fit them to several Gaussian vibronic lines to determine the 0−0 transition.[3,11,29,33,34] To compare the line shape of our β-carotene TPE spectrum to the line shape of the β-carotene S_1 fluorescence spectrum measured by Koyama,[29] we simply take the mirror image of the fluorescence spectrum as shown in Figure 6. Koyama and co-workers determined the 0−0 transition of S_1 state for β-carotene to be 14500 cm^{-1}.[29] The TPE spectrum only covers the red portion of the S_1 spectrum. The agreement between the TPE spectrum and the mirror image of the fluorescence spectrum with one-photon excitation is good. Unfortunately there is no measurement of the fluorescence spectrum of lutein from the S_1 state. On the basis of vioxanthin and zeaxanthin fluorescence results,[11] the range of the TPE spectrum for lutein also appears to be limited to the red part of S_1-S_0 absorption spectrum.

In Figure 6c the TPE spectrum of LHC II, observed by monitoring the chlorophyll fluorescence, is plotted.[46] The onset of this spectrum is significantly blue shifted to $\sim 15100 \pm 300$ cm^{-1} compared to Cars in solution. The width of the spectrum is also narrower than that in solution. The TPE spectrum was

also measured with a LHC II sample from spinach. The spectrum showed no significant difference from that of *C. reinhardtii*.[46] The pump−probe data obtained from the Cars in solution have poorer signal-to-noise ratio than the LHC II data because of the different detection methods. Nevertheless, the large blue shift and narrower spectrum obtained in LHC II has important implications for the role of these carotenoids in light-harvesting proteins of plants. Comparison of Figure 6c with Figure 6a and 6b indicates that the energy transferring Car states in LHC II have substantially higher energies than lutein in solution. This is significant since lutein is the most abundant carotenoid (∼60%) in LHC II.

4. Discussion

In our discussion of the results obtained in this and previous work, we will focus on the differences between the spectral line shape obtained by one-photon measurements in solution and two-photon excitation measurements in solutions and proteins and also the differences in the conclusions drawn about the Car S_1 state in LHC II from two-photon experiments and some one-photon pump−probe experiments.[5,17] In our opinion the two most striking differences in these studies are (i) the very different TPE-spectrum of the Car S_1 states in LHC II compared to Cars in solution and (ii) the very different time-scales given for the Car $S_1 \rightarrow$ Chl EET. The former point is very important for the determination of the energy levels of the Car S_1 states in LHC II and of which Cars transfer energy efficiently from their S_1 states. The location of the Car energy levels also has important implications for the role of the Car S_1 state in the so-called nonphotochemical quenching process of higher plants.[10,13,25,33]

4.1. Comparison of Our Results with the One-Photon Excitation Spectra. Our TPE spectrum of the Car S_1 state in LHC II has a very different line shape from either the mirror image of the S_1 fluorescence spectrum or the TPE spectrum of typical carotenoids observed in solution (compare Figure 6a−c). Carotenoids in LHC II consist of lutein, violaxanthin, and neoxanthin. Frank and co-workers measured the S_1 fluorescence of violaxanthin in *n*-hexane.[11] The width of the fluorescence spectrum of violaxanthin seems to be narrower than that of β-carotene, but the quantitative estimation of the width is difficult since the red tail of the fluorescence spectrum was not reported. A comparison with lutein is of importance since it is the most abundant Car in LHC II (∼60%). Our TPE spectrum in LHC II is exceptionally blue-shifted compared to our TPE spectrum of lutein in solution.

There are several possibilities to explain the difference in line shapes between LHC II and the solution spectra. It may be related to a difference in Franck−Condon factors in the two measurements. Comparison of the one-photon and two-photon fluorescence excitation spectra of short polyenes suggests that there is a difference of about 100 cm^{-1} between the one-photon and two-photon spectral origins if the molecule has inversion symmetry.[30,31] The pattern of Franck−Condon progressions for two-photon excitation spectrum is, however, the same as that for one-photon excitation. For one-photon excitation, the 0−0 transition is built on nontotally symmetric (b_u) vibrational modes starting from a false origin. These vibrational modes are in-plane bending modes with frequencies of about 100 cm^{-1}. If a molecule does not have inversion symmetry, the 0−0 transition is weakly allowed even though bands built on the vibronic origin dominate the one-photon spectrum. Because there are the same vibrational progressions in the one- and two-photon fluorescence spectra (with the only difference between the two being a shift in the vibrational origin), we conclude that the spectral differences between one- and two-photon excitation are not due to differences in Franck−Condon factors for the two excitation methods.

The TPE spectrum of LHC II was measured by exciting the Car S_1 transition and monitoring fluorescence from the Chl. If Chl transitions were to contribute to the observed TPE spectrum, the shape of the TPE spectrum would be distorted. In previous papers, we considered the possibility that one-photon allowed Chl states in the visible region contribute to the TPE spectrum via two-photon absorption.[23,46] We concluded that the contribution of Chls in the TPE spectrum is at least 20 times smaller than that of Cars. We now consider possible one-photon transitions in the near-infrared region. Even though there is no allowed Chl transition in near-infrared region, the spin-forbidden T_1-S_0 transition of Chl is located in this region, which might contribute to the measurement. However, the location of the T_1-S_0 transition was determined to be around 970 nm, which is shorter than our pump wavelength (1000−1600 nm).[42] Therefore, direct excitation of the triplet state is very unlikely in the case of Chl (as opposed to BChl) since its T_1 energy is slightly higher than our pump energy.[42]

One might also consider the possible contribution of the B_u^- state to the TPE spectrum. The transition to this state is one- and two-photon forbidden, so here we consider the possibility of thermal excitation from the S_1 state. According to Koyama et al., the B_u^- state is 3950, 3400, 2570, 2400, 1880, and 1700 cm^{-1} above the S_1 state for mini-9-β-carotene (the number of conjugated double bonds, n=9), spheriodene ($n = 10$), lycopene ($n = 11$), anhydrorhodovibrin ($n = 12$), β-carotene ($n = 11$), and spirilloxanthin ($n = 13$), respectively.[14,38,39] Since LHC II contains Cars with 9 or 10 conjugated double bonds, we can assume that their B_u^- state energies lie about 3500 cm^{-1} above their S_1 state energies in accordance with the above trend. Thermal energy at room temperature is about 200 cm^{-1}, which is an order of magnitude too small to thermally excite the B_u^- state. So, we conclude that the B_u^- state does not contribute to the TPE spectra of the Cars examined in this work.

Figure 6b and the results of Sundström and co-workers suggest that the Car S_1 0−0 transitions of lutein, zeaxanthin (14030 cm^{-1}), and violaxanthin (14470 cm^{-1}) are below the 0−0 transition of the lowest Chl Q_y states (∼14700 cm^{-1}).[33] If this is indeed the case, EET is energetically only possible from hot Car states that are above the 0−0 transition of the lowest Chl Q_y states. However, the placement of the Car S_1 energies below the Chl Q_y states is still controversial since resonance-Raman[38−40] and fluorescence[11,15] measurements obtain S_1 energy values that are systematically 400−800 cm^{-1} higher than those obtained by the IR pump−probe technique of Sundström and co-workers mentioned above. If the Car S_1 energies are below or even approximately isoenergetic with the Chl Q_y states, EET from hot states can explain the relatively narrow two-photon fluorescence excitation spectrum of the Car S_1 states in LHC II since this spectrum captures only those Car energy levels involved in EET, i.e., those with energies above the lowest Chl Q_y states. We will discuss this issue in terms of the time scales of EET in next section. However, in this model, we cannot explain the difference of the spectra on the blue side.

To compare the line shape of the TPE spectrum in the LHC II protein with that of the S_1 fluorescence spectra in solution, we have to make three assumptions. One assumption is that the shape of the absorption spectrum is simply the mirror image of the fluorescence spectrum. Second, we assume that the Stokes shift of the S_1 state of carotenoids is small. The third assumption is that the shape of the spectrum in protein is the same as that

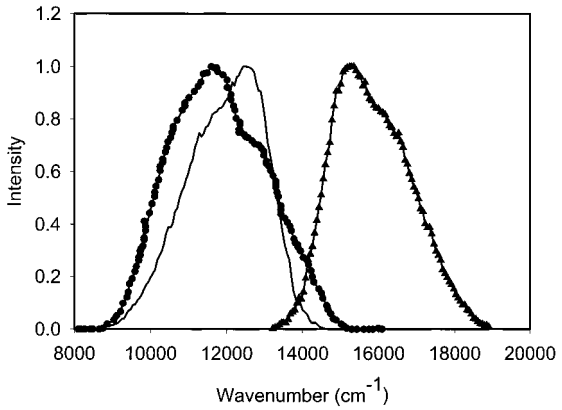

Figure 7. Comparison of one-photon and two-photon spectra of spheroidene. One-photon fluorescence spectrum of spheroidene in solution (circles).[15] TPE spectrum of spheroidene in LH2 protein from *Rb. sphaeroides* monitored by BChl fluorescence (solid line with triangles).[23] Mirror image of the TPE spectrum (solid line).

in solution. It is well-known that these assumptions are reasonable for the absorption and fluorescence spectra of the Car S_2 state in solution and proteins. However it is not straightforward to apply these assumptions to the Car S_1 state since the nature of the S_1 and S_2 electronic states is very different.

As a point of comparison, Figure 7 shows the TPE spectrum of spheroidene in light harvesting complex 2 (LH2) from *Rhodobacter sphaeroides* along with its mirror image, which can be compared to the one-photon fluorescence spectrum of spheroidene in solution. The TPE-spectrum for spheroidene has a very similar 0−0 transition in the LH2 protein and in solution.[23] Generally the S_1 energies of carotenoids do not depend strongly on the solvent polarizability since the covalent $2A_g^-$ state has a lower polarizability than the $1B_u^+$ state. However, the line shapes of the TPE mirror image (spheroidene in LH2) and the fluorescence spectrum (spheroidene in solution) are noticeably different: the bandwidth of the TPE spectrum is slightly narrower than the one-photon fluorescence, and the vibrational bands have different relative intensities in the two spectra. These differences may be due to solvent effects, and/or the fluorescence spectrum may not be well approximated by the mirror image of the TPE absorption spectrum**.** To evaluate the accuracy of the mirror image approximation, the absorption and fluorescence spectra of several dozen aromatic molecules in solution were considered.[2] Chromophores with weak electronic transitions tend to show noticeable differences in line shape between their absorption and fluorescence spectra. These line shape differences are of the same magnitude as those seen here between the mirror image of the TPE spectrum of spheroidene in LH2 and the fluorescence spectrum of spheroidene in solution. Therefore, we consider the agreement to be as good as might be reasonably expected.

In considering solvent effects on spectral line shapes, a recent study by Sundström and co-workers is relevant. Near-infrared transient absorption spectroscopy was used to determine the energy of the S_1 state (prepared via S_2 excitation) of the carotenoid spheroidene in *n*-hexane.[34] The energy of this state was found to be 13400 cm^{-1}, which is 800 cm^{-1} lower than the values obtained from previous fluorescence and resonance Raman measurements.[15,40] They suggested that the difference could be explained in terms of different conformational species, with significantly different energies, coexisting in the S_1 state. The crystal structures of the LH2 complexes from the purple bacteria *Rps. acidophila* and *Rs. molischianum* show that the carotenoid is distorted by the protein environment. Such a structural deformation should affect the energy level and vibronic structure of the S_1 state and increase the S_1-S_0 oscillator strength via S_1-S_2 mixing.[20] It is, thus, not unreasonable to expect different shapes of the S_1 spectra in solution and in proteins. Clearly, a direct measurement of the S_1 excitation and fluorescence spectra in proteins is necessary to characterize the energetics of the Car S_1 state and the vibronic structure of the S_1 spectrum.

4.2. Different Time Scales for Car S_1-Chl EET for One-Photon and Two-Photon Excitation. In this section we will address the different time scales for Car S_1-Chl EET between one-photon pump−probe experiments and fluorescence up-conversion experiments with two-photon excitation.[5,17,46] Recently van Amerongen and co-workers and Holzwarth and co-workers[5,17] used femtosecond transient absorption spectroscopy to obtain spectral and kinetic information on energy transfer from Car to Chl in LHC II and CP29. They concluded that the main contribution to Car $S_1\rightarrow$ Chl EET comes from lutein and approximately 15−20% of the initial Car excitations are transferred to Chls with a time constant of around 1 ps from the Car S_1 state. For fluorescence up-conversion measurements, we can only monitor the population of the Car S_1 state which causes the energy transfer to Chl. If energy transfer occurs from vibrationally hot Car S_1 states, this could explain the observed fast Car $S_1\rightarrow$Chl EET time constant. After photoexcitation, a nonthermal energy distribution in the vibrational levels is created. Intramolecular vibrational relaxation (IVR) distributes energy among many degrees of freedom and is then followed by a vibrational cooling process. In our case, ultrafast IVR to vibrationally relaxed S_1 states provides only a very short time window for Car $S_1\rightarrow$Chl EET (see Figure 2). However, if such an EET pathway contributes significantly, the EET time constant τ_{ET1} has to be at least competitive with the typical time scales for vibrational relaxation. The feasibility for an overall sub-picosecond Car $S_1\rightarrow$Chl EET in LHC II for Car states with an energy higher than >15300 cm^{-1} has already been shown in our previous paper.[46] It is simply a result of the large number of acceptor Chl molecules in van der Waals contact with the central Car. In the case of LHC II, primarily lutein and some neoxanthin occupy the central positions that are surrounded by Chls, making them the most likely energy transferring Cars to account for the fast EET, though a role for violaxanthin, especially in the LHC II trimer, cannot be ruled out. The additional slow ps Car $S_1\rightarrow$Chl EET time constants obtained in the present work can be attributed to low efficiency EET from relaxed Car states that are just below or above the lowest Chl Q_y states because the spectral overlap for these states is very poor. This explanation is consistent with all the experimental results and is probably of significance for EET from higher states of other pigments (e.g., from hot Chl Q_x or Chl *b* states after IC from the Chl Soret level).[26]

Calculations of rate constants for electronic excitation transfer in the weak coupling limit are usually based on the Förster expression, which is a form of the Fermi Golden Rule:[8,9]

$$k_{ET} = \frac{2\pi}{\hbar}|V|^2 J_{DA} \qquad (2)$$

According to this theory, the rate for EET between a donor and an acceptor is proportional to the density of energy-conserving states, which can be approximated by the spectral overlap integral of donor fluorescence $f_D(\nu)$ and acceptor absorption, $\epsilon_A(\nu)$ and the square of the electronic coupling constant *V*,

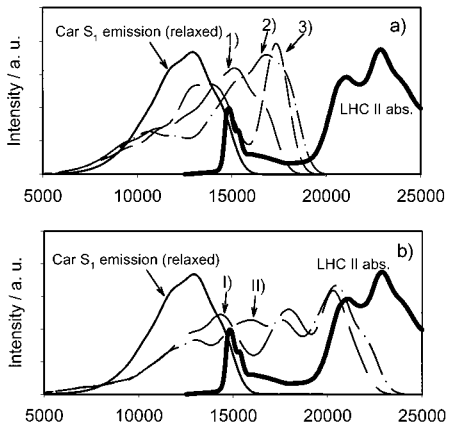

Figure 8. (a) Car S_1 emission spectra from various hot states corresponding to two quanta excited (dashed−dotted lines). The solid line shows the relaxed fluorescence spectrum. The hot spectrum was calculated with the model described in the text and the parameters of Tables 2 and 3. The absorption spectrum of LHC II is also shown (thick solid line). (b) Car S_1 emission spectra from various hot states corresponding to five quanta excited (dashed−dotted lines). The thick solid line shows the relaxed fluorescence spectrum. The hot spectrum was calculated with the model described in the text and the parameters of Tables 2 and 3. The absorption spectrum of LHC II is also shown (thick solid line).

which, of course, depends on the nature of the underlying EET mechanism.[18,42,43]

$$J_{DA} = \frac{\int f_D(\nu)\epsilon_A(\nu)\,d\nu}{\int f_D(\nu)\,d\nu \int \epsilon_A(\nu)\,d\nu} \qquad (3)$$

The spectral overlap of the Car S_1 donor emission with the Chl *a* acceptor absorption would be small if the Cars have a 0−0 transition of <15000 cm^{-1} as suggested by the experimental results for lutein in solution (Figure 6b).[33] This allows only very slow uphill EET via thermal excitation. Overlap with Chl *b*, which is higher in energy than Chl *a*, would be even poorer thus precluding any significant EET from the Car S_1 states.

To illustrate energy transfer from vibrationally hot states, we present some model calculations. The method of calculation of the spectra in Figure 8 has been described in detail.[28] Briefly, they were calculated within the framework of the Born−Oppenheimer approximation by considering only the dominant high-frequency Franck−Condon active vibrational modes with energies larger than k_BT. These modes are mainly the C−C and C═C-stretch vibrations of carotenoids.[29,40] Low-frequency modes cause line broadening, which is described by a Gaussian line shape.[29] To calculate the Franck−Condon intensity of the modes, their potential curves in the ground and excited states have been treated in the harmonic approximation. The dimensionless displacement of the harmonic potentials Δ of each mode is not known. Furthermore we do not have any information on how these parameters change in protein complexes. Therefore we used parameters for β-carotene in solution obtained by Koyama and co-workers.[29] The frequency of C−C stretching mode is set to be 1160 cm^{-1} both in the $1A_g^-$ and $2A_g^-$ states. Due to the presence of vibronic coupling between the $1A_g^-$ and $2A_g^-$ states, the frequency of C═C stretching mode in the $2A_g^-$ state is 1780 cm^{-1} whereas in the $1A_g^-$ state it is 1520 cm^{-1}. The parameters used for the calculations are summarized in Tables 2 and 3. Of course, there are uncertainties in the calculations due to limited knowledge of the necessary parameters. Nevertheless, the results give a qualitative picture, which we expect to resemble the actual situation. Varying the parameters in Table 2 over a reasonable range produces similar results.

TABLE 2: High-Frequency Modes Used for the Calculation of the Hot Spectra

mode	ω_g (cm^{-1})[a]	ω_e (cm^{-1})[a]	dimensionless displacement
1	1160	1160	1.52
2	1520	1780	1.63

[a] ω_g refers to the ground-state frequency and ω_e is the excited-state frequency. Line broadening is described by Gaussian function with a width of 1500 cm^{-1} fwhm.

TABLE 3: Quantum Numbers Used for the Calculation of the Hot Spectra

plot in Figure 7	quanta in 1160 cm^{-1} mode	quanta in 1780 cm^{-1} mode
(1)	2	0
(2)	0	2
(3)	1	1
(I)	3	2
(II)	2	3

Figure 8a shows the calculated donor emission spectrum, which represents the emission after exclusive excitation of the vibronic states (two quanta in the high-frequency modes, thin lines 1−3 in Figure 8) excited by the two-photon excitation wavelength chosen in our earlier TPE-upconversion study of LHC II.[46] In this experiment we excited at $\sim$16800 cm^{-1}, which is about two $\sim$1100 cm^{-1} quanta higher than the 0−0 transition estimated from Figure 5b ($\sim$14350 cm^{-1}). It is obvious that the spectral overlap is excellent and can explain very efficient EET before vibrational relaxation is complete.

In nature, the Car S_2 state is initially populated, followed by rapid Car $S_2 \rightarrow$ Car S_1 IC on a time scale of 100−200 fs, which creates hot Car S_1 states. It is unknown which vibronic levels will be populated from this IC, so the simulated spectra should be viewed as a qualitative model. However, if all of the S_2 state energy were to go into S_1 vibrational modes, no more than five quanta of the 1200 cm^{-1} mode could be created. In Figure 8b, calculated emission spectra are shown for different population distributions of five quanta in the two stretching modes (thick dashed lines I and II in Figure 8).

The corresponding overlaps demonstrate that we can expect a strongly multiexponential behavior of the sub-picosecond EET kinetics during IVR.[5,17] Koyama and co-workers also suggested the enhancement of the energy transfer efficiency via higher vibronic states.[48] Indeed, they found that the vibrational relaxation in the S_1 state of all-trans-lycopene takes place more slowly than internal conversion to the S_0 state (5−6 ps).[48] Since the typical time constants observed for EET in LHC II are on the order of 100 fs, we believe that a very similar situation also applies to EET kinetics after initial excitation of the Chl Soret or Chl Q_x states. A consequence of this assumption is that it does not make sense to assign experimentally observed time constants to EET between a few levels of individual states because the time constants fitted to the experimental results only represent averaged values describing the multiexponential kinetics.

The Cars in LHC II may have S_1 0−0 transitions at or below 15000 cm^{-1}. The TPE-spectrum of LHC II, detected by Chl fluorescence, must drop to zero below 15000 cm^{-1} because the lowest vibronic levels of the Cars have no significant spectral overlap with the acceptor states of the Chls below this energy

(see Figure 8a). Therefore, even efficient TPE to the Car S_1 cannot be monitored for this wavelength range by detecting the Chl fluorescence, and the "real" TPE-spectrum of the Cars is then cut off at this frequency.

5. Conclusion

The pump−probe kinetics of the Car S_1 state in LHC II after one-photon excitation of Car S_2 show three time scales of ∼200 and 700 fs and >2−8 ps. The very short lifetimes correspond to Car states, from which efficient Car S_1→Chl EET occurs. The slower lifetimes correspond to Car states with inefficient Car S_1→Chl EET. Only the fast EET time constant was seen in our previous TPE fluorescence upconversion experiment[46] because this particular experiment is dependent on efficient Car S_1→Chl EET. To determine the TPE spectrum of the Car S_0→Car S_1 transition of Cars in solution, we performed femtosecond two-photon pump−probe measurement by monitoring the Car S_1→Car S_n ESA as a function of the two-photon pump frequency. The resulting TPE-spectra suggest that the 0−0 transition of lutein, the most abundant Car in LHC II, has a Car S_1 energy below the lowest Chl-levels. Although resonance-Raman[38−40] and fluorescence[11,15] experiments obtain higher values for Car S_1 energies, a recent study of Sundström and co-workers also suggests that other Cars in LHC II have S_1 energies below the lowest Chl-levels.[33] Furthermore, the width of the TPE spectrum is narrower than that expected from the S_1 fluorescence of Car in solution. We propose a simple model to account for these findings that allows for Car S_1→Chl EET via hot Car S_1 states. This model shows that sub-picosecond EET from hot Car S_1 states is feasible. In nature, hot states of Car S_1 are always initially created via the Car S_2→Car S_1 IC from the optically allowed Car S_2 state. We estimate that, during the vibrational relaxation, about 50% of the Car S_1 population could be transferred to the Chls.

Acknowledgment. This work was supported by the Director, Office of Science, of the U.S. Department of Energy under Contract No. DE-AC03-76SF00098. We thank Professor R. L. Christensen and Professor L. D. Ziegler for valuable discussions, and Professor K. K. Niyogi for HPLC analysis. P.J.W. is grateful for financial support from the Deutsche Forschungsgemeinschaft. K.O. is a Japanese Society for the Promotion of Science (JSPS) Research Fellow.

References and Notes

(1) Agarwal, R.; Krueger, B. P.; Scholes, G. D.; Yang, M.; Yom, J.; Mets, L.; Fleming, G. R. *J. Phys. Chem. B* **2000**, *104*, 2908−2918.

(2) Berlman, I. B. *Handbook of Fluorescence Spectra of Aromatic Molecules*, 2nd ed.; Academic Press: New York, 1971.

(3) Chynwat, V.; Frank, H. A. *Chem. Phys* **1995**, *194*, 237−244.

(4) Comment. In *Chlamydomonas reinhardtii*, the very similar carotenoid, loroxanthin, occupies about 30% of the sites usually filled by lutein in other organisms.

(5) Connelly, J. P.; Müller, M. G.; Bassi, R.; Croce, R.; Holzwarth, A. R. *Biochemistry* **1997**, *36*, 281−287.

(6) Croce, R.; Remelli, R.; Varotto, C.; Breton, J.; Bassi, R. *FEBS Lett.* **1999**, *456*, 1−6.

(7) Croce, R.; Weiss, S.; Bassi, R. *J. Biol. Chem.* **1999**, *274*, 29613−29623.

(8) Forster, T. *Ann. Phys.* **1948**, *2*, 55.

(9) Förster, T. Delocalized Excitation and Excitation Transfer. In *Modern Quantum Chemistry*; Academic Press: New York, 1965; Vol. III, pp 93−137.

(10) Frank, H. A.; Bautista, J. A.; Josue, J.; Pendon, Z.; Hiller, R. G.; Sharples, F. P.; Gosztola, D.; Wasielewski, M. R. *J. Phys. Chem. B* **2000**, *104*, 4569−4577.

(11) Frank, H. A.; Bautista, J. A.; Josue, J. S.; Young, A. J. *Biochemistry* **2000**, *39*, 2831−2837.

(12) Frank, H. A.; Cogdell, R. J. *Photochem. Photobiol.* **1996**, *63*, 257−264.

(13) Frank, H. A.; Cua, A.; Chynwat, V.; Young, A.; Gosztola, D.; Wasielewski, M. R. *Photosynth. Res.* **1994**, *41*, 389−395.

(14) Fujii, R.; Ishikawa, T.; Koyama, Y.; Taguchi, M.; Isobe, Y.; Nagae, H.; Watanabe, Y. *J. Phys. Chem. A* **2001**, *105*, 5348−5355.

(15) Fujii, R.; Onaka, K.; Kuki, M.; Koyama, Y.; Watanabe, Y. *Chem. Phys. Lett.* **1998**, *288*, 847−853.

(16) Gillbro, T. Unpublished Results.

(17) Gradinaru, C. C.; van Stokkum, I. H. M.; Pascal, A. A.; van Grondelle, R.; van Amerongen, H. *J. Phys. Chem. B* **2000**, *104*, 9330−9342.

(18) Hobe, S.; Niemeier, H.; Bender, A.; Paulsen, H. *Eur. J. Biochem* **2000**, *267*, 616−624.

(19) Horton, P.; Ruban, A. V.; Walters, R. G. *Annu. Rev. Plant Physiol. Plant Mol. Biol.* **1996**, *47*, 655−684.

(20) Hsu, C.-P.; Walla, P. J.; Head-Gordon, M.; Fleming, G. R. *J. Chem. Phys.* **2001**. Submitted for publication.

(21) Jansson, S. *Biochim. Biophys. Acta, Bioenergetics* **1994**, *1184*, 1−19.

(22) Jennings, R. C.; Bassi, R.; Zucchelli, G. *Top. Curr. Chem.* **1996**, *177*, 147−181.

(23) Krueger, B. P.; Yom, J.; Walla, P. J.; Fleming, G. R. *Chem. Phys. Lett.* **1999**, *310*, 57−64.

(24) Kühlbrandt, W.; Wang, D. N.; Fujiyoshi, Y. *Nature* **1994**, *367*, 614−621.

(25) Moya, I.; Silvestri, M.; Cinque, G.; Bassi, R. Preprint **2001**.

(26) Mukamel, S.; Rupasov, V. *Chem. Phys. Lett.* **1995**, *242*, 17−26.

(27) Nagae, H.; Kuki, M.; Zhang, J. P.; Sashima, T.; Mukai, Y.; Koyama, Y. *J. Phys. Chem. A* **2000**, *104*, 4155−4166.

(28) Ohta, K.; Kang, T. J.; Tominaga, K.; Yoshihara, K. *Chem. Phys.* **1999**, *242*, 103−114.

(29) Onaka, K.; Fujii, R.; Nagae, H.; Kuki, M.; Koyama, Y.; Watanabe, Y. *Chem. Phys. Lett.* **1999**, *315*, 75−81.

(30) Petek, H.; Bell, A. J.; Choi, Y. S.; Yoshihara, K.; Tounge, B. A.; Christensen, R. L. *J. Chem. Phys.* **1993**, *98*, 3777−3794.

(31) Petek, H.; Bell, A. J.; Choi, Y. S.; Yoshihara, K.; Tounge, B. A.; Christensen, R. L. *J. Chem. Phys.* **1995**, *102*, 4726−4739.

(32) Peterman, E. J. G.; Calkoen, F.; Gradinaru, C.; Dukker, F. M.; van Grondelle, R.; van Amerongen, H. In *Photosynthesis: from Light to Biosphere*; Kluwer Academic Publishers: Dordrecht, 1995; Vol. IV, pp 31−34.

(33) Polivka, T.; Herek, J. L.; Zigmantas, D.; Akerlund, H. E.; Sundstrom, V. *Proc. Natl. Acad. Sci. U. S. A* **1999**, *96*, 4914−4917.

(34) Polivka, T.; Zigmantas, D.; Frank, H. A.; Bautista, J. A.; Herek, J. L.; Koyama, Y.; Fujii, R.; Sundstrom, V. *J. Phys. Chem. B* **2001**, *105*, 1072−1080.

(35) Rogl, H.; Kuhlbrandt, W. *Biochemistry* **1999**, *38*, 16214−16222.

(36) Ruban, A. V.; Lee, P. J.; Wentworth, M.; Young, A. J.; Horton, P. *J. Biol. Chem.* **1999**, *274*, 10458−10465.

(37) Ruban, A. V.; Young, A. J.; Horton, P. *Biochemistry* **1996**, *35*, 674−678.

(38) Sashima, T.; Koyama, Y.; Yamada, T.; Hashimoto, H. *J. Phys. Chem. B* **2000**, *104*, 5011−5019.

(39) Sashima, T.; Nagae, H.; Kuki, M.; Koyama, Y. *Chem. Phys. Lett.* **1999**, *299*, 187−194.

(40) Sashima, T.; Shiba, M.; Hashimoto, H.; Nagae, H.; Koyama, Y. *Chem. Phys. Lett* **1998**, *290*, 36−42.

(41) Siefermann-Harms, D. *Biochim. Biophys. Acta, Bioenergetics* **1985**, *811*, 325−355.

(42) Takiff, L.; Boxer, S. G. *J. Am. Chem. Soc.* **1988**, *110*, 4425−4426.

(43) van Grondelle, R.; Dekker: J. P.; Gillbro, T.; Sundstrom, V. *Biochim. Biophys. Acta, Bioenergetics* **1994**, *1187*, 1−65.

(44) Walla, P. J.; Linden, P. A.; Fleming, G. R. Fs-Transient Absorption and Fluorescence Upconversion after Two-photon Excitation of Carotenoids in Solution and in LHC II. In *Ultrafast Phenomena*; Elsaesser, T., Mukamel, S., Murnane, M. M., Scherer, N. F., Eds.; Springer: New York, 2000; pp 671−673.

(45) Walla, P. J.; Linden, P. A.; Hsu, C.-P.; Scholes, G. D.; Fleming, G. R. *Proc. Natl. Acad. Sci. U. S. A* **2000**, *97*, 10808−10813.

(46) Walla, P. J.; Yom, J.; Krueger, B. P.; Fleming, G. R. *J. Phys. Chem. B* **2000**, *104*, 4799−4806.

(47) Wasielewski, M. R.; Kispert, L. D. *Chem. Phys. Lett.* **1986**, *128*, 238−43.

(48) Zhang, J. P.; Chen, C. H.; Koyama, Y.; Nagae, H. *J. Phys. Chem. B* **1998**, *102*, 1632−1640.